

Morphology, Microstructure Evolution and Properties of Resin-Bonded Palm Kernel and Coconut Shell Grain-Based Abrasive Grinding



A. A. Samuel¹, A. Sulaiman², H. A. Ajimotokan^{2*}, S. E. Ibitoye², T. K. Ajiboye², T. S. Ogedengbe¹, I. O. Alabi³

¹Department of Mechanical Engineering, Nile University, Abuja, Nigeria

²Department of Mechanical Engineering, University of Ilorin, Ilorin, Nigeria

³Department of Mechanical Engineering, Elizade University, Ilara-Mokin, Nigeria



ABSTRACT: This study examined the morphology and microstructural evolution of resin-bonded palm kernel and coconut shell grain-based abrasive grinding wheels and their physico-mechanical and tribological properties. Raw palm kernel shell (PKS) and coconut shell (CNS) samples were obtained, sorted, sun- and oven-dried, pulverised, and screened into fines of 250, 500 and 850 μm grain sizes, and blended at PKS to CNS mixing ratios of 1:0, 0:1, 1:2, 1:1 and 2:1, respectively. The blended grains, on a weight basis of the total aggregates, were bonded with 25 wt.% polyester resin and hardened and catalysed with 1.5 wt.% cobalt compound and methyl-ethyl ketone peroxide. The aggregates were moulded and compressed at a constant pressure of 18 MPa, ejected, and room-cured before being oven-cured to produce the wheels. The microstructural, water absorption, impact, flexural, hardness, and wear rate properties of the produced samples were evaluated. The properties studied were significantly influenced by grain sizes and mixing ratios of the PKS and CNS in the wheels. The least hardness value, 6.42 HRB, and wear rate, 0.44 mg/m were found in wheels produced from aggregates with pure PKS content with 850 and 250 μm grain sizes, respectively. The wheels' durability qualities suggest they could be used as abrasive grinding wheels, in particular, for wood cutting and finishing processes.

KEYWORDS: Agro-residues; Grain-based abrasives; Abrasive grinding wheels; Performance matrices.

[Received Jul. 20, 2022; Revised Nov. 4, 2022; Accepted Jan 4, 2023]

Print ISSN: 0189-9546 | Online ISSN: 2437-2110

I. INTRODUCTION

Health and environmental concerns about non-biodegradable crude oil-derived phenolic- or thermoplastic-based frictional-filler or abrasive materials, as well as their rising cost, have renewed interest in commonly underexploited biodegradable agro-residues as promising alternative and renewable abrasive materials (Ajimotokan *et al.*, 2022; Ajimotokan & Samuel, 2020; Sauget, Zhou, & Pizzi, 2014; Senthilkumar *et al.*, 2018; Suresh, Sudhakara, & Vinod, 2020; Zhang *et al.*, 2015). Furthermore, abrasive materials made from oil-derived phenolic or thermoplastic-based materials have poor performance and oxidation resistance at high temperatures, which are disadvantages in their use (Ajimotokan & Samuel, 2020; Zhang *et al.*, 2015). As a result of these disadvantages, significant efforts are being made to develop innovative manufacturing processes for producing abrasives from alternative and renewable materials (Ajimotokan & Samuel, 2020).

Abrasives are minute, hard particles with irregular shapes and sharp edges that are used to wear and cut off the surface of softer, less resistant materials (Ratia *et al.*, 2014). Natural and synthetic abrasives, which can be made from a variety of

materials, can be used as abrasives (Durowaye, Lawal, Akande, & Durowaye, 2014; Kohli, 2016; Zhan, Wang, & Wang, 2021). Strength, hardness, wear resistance, thermochemical stability, and sharp cutting points are all characteristics of these materials (Obot, Yawas, & Aku, 2017). Largely, one of the commonly used alternative and renewable organic materials, as abrasives, are grains from agro-residues (Ajimotokan & Samuel, 2020; Samuel, 2019). Commercially generated agro-residues, also known as agricultural or crop residues, such as palm kernel, coconut, snail, and periwinkle shells, can be used as suitable abrasives for abrasive grinding wheel production (Ajimotokan *et al.*, 2022; Ajimotokan & Samuel, 2020; Tegegne & Shiferaw, 2020).

Grinding wheels, also known as grinding discs are wheels made from abrasive materials or compounds, employed for various fine grinding, in particular, finish machining processes; and most broadly for abrasive cutting and machining operations (Bratan, Roshchupkin, & Novikov, 2017). Generally, the wheels are made from non-biodegradable composite materials, comprising aggregate of coarse-particles, compressed and bonded with a cementing matrix, forming circular shaped solids of different profiles and cross sections, on the basis of the wheel's anticipated usage

*Corresponding author: hajims@unilorin.edu.ng,

(Godino *et al.*, 2018). Also, they can be formed on a solid steel or aluminium disc surface with the abrasive grains bonded onto it (Zhang *et al.*, 2015).

Samuel, (2019) developed coconut and palm kernel shell abrasive grinding wheels and investigated their physico-mechanical properties. Raw samples of CNS and PKS were collected, sorted and pulverised into particles of 0.25 mm, 0.5 mm and 0.85 mm particle sizes. The particles were blended at mixing ratios of 1:0, 1:1, 2:1, 1:2 and 0:1 CNS to PKS; bonded with 25% of resin as binder on a weight basis while 0.7% cobalt compound and methyl-ethyl ketone peroxide were used as the hardener to initiate polymerization and catalyse the reaction process, respectively. The author reported that the resulting durability qualities of the wheels made from CNS and PKS suggest that they could be used for grinding purposes.

Similarly, Obot, Yawas and Aku, (2017) developed an abrasive material employing the shells of periwinkle. Raw periwinkle samples were obtained, sorted and pulverised into FEPA grit standards before being screened into P40, P60, and P140 grits. The fine grains were developed into polymer matrix composites by blending grains in varying range of 87 wt.% to 95 wt.% with resin contents in the varying range of 4 wt.% to 12 wt.% and 0.5 wt.% of each cobalt naphthalene and methyl ethyl ketone peroxide, the fine grains were developed into polymer matrix composites and poured and moulded using a hydraulic press. The authors reported that as resin content increased, hardness and compressive strength also increased while wear rate fell. The admixture made using the 12 wt.% resin-bonded 87 wt.% periwinkle shell grains for all grain sizes had the best abrasiveness properties.

Another study by Zhang *et al.*, (2015) developed and assessed the physico-mechanical characteristics of glass sand and bioresin matrix abrasive grinding wheels. Condensed tannin-furanic resin, derived from biosourced raw agro-products, was used to create the raw resin matrix, which served as the foundation for the grinding wheel made of biobased thermosetting resins. According to the authors, the results were on par with those of commercial grinding wheels made from grains of aluminium oxide and synthetic phenolic resin. These results suggested that these novel tannin-based grinding wheels could be used to achieve an unmatched hardness and tough resistance with regard to compression. Additionally, they displayed exceptional abrasive qualities that outperformed those of the widely available H-18 Taber Calibrade grinding wheel.

Numerous studies have also been conducted to examine and evaluate the physico-mechanical and tribological characteristics of biosourced abrasive grinding wheels in relation to their usage circumstances. On the basis of this background, this study examines the morphology and microstructure evolution of resin-bonded palm kernel and coconut shell grain-based grinding wheels and their physico-mechanical and tribological properties.

II. MATERIALS AND METHODS

Raw samples of palm kernel shell (PKS) and coconut shell (CNS) were collected in the Nigerian towns of Ila Orangun, Ila and Oja-Oba, Ilorin, respectively; and labelled

appropriately. The polyester resin (i.e. the binder), cobalt naphthalene (i.e. the hardener) and methyl-ethyl ketone peroxide (i.e. the catalyst) were obtained from Ojota, Lagos, Nigeria. The raw PKS and CNS samples were sorted, sun- and oven-dried, pulverised and sieved into fines of 250, 500 and 850 μm grain sizes, and afterwards, blended at mixing ratios of 1:0, 0:1, 1:2, 1:1 and 2:1 for PKS and CNS, respectively. The sieve into fines was carried out using mechanical sieve by Gibson International with standard sizes of 8 in, 10 in, and 12 in, respectively for the 250, 500, and 850 μm grain sizes. The blended grains, on a weight basis of the total aggregates, were bonded with 25 wt.% polyester resin, hardened with 1.5 wt.% cobalt naphthalene to initiate polymerisation, and catalysed with 1.5 wt.% methyl-ethyl ketone peroxide to speed up the reaction process; poured into prepared moulds, and then moulded at a constant compacting pressure of 18 MPa using a hydraulic compression machine. The resulting resin-bonded palm kernel and coconut shell grain-based grinding wheels were carefully ejected, and cured at room temperature for 20 days, and then, oven-cured at 100°C for 2 hours. The microstructure, water absorption, impact, flexural, hardness, and wear rate properties of the produced grinding wheels were evaluated.

A. Materials preparation and formulation

The raw PKS and CNS were sorted by handpicking to remove foreign materials, washed with water to remove dust and dirt, sun-dried for five days, and subsequently, oven-dried at 100°C for 4 hours for moisture reduction. The raw samples were then pulverised using a 3,730 W hammer mill and screened into 250, 500 and 850 μm grain sizes according to the standard procedures of ASTM 11-20 (ASTM E11-20, 2020) and the Federation of European Producers of Abrasives (FEPA) (FEPA, 2020) to categorise the grains into grits of F30, F36 and F60, respectively.

A digital weighing balance was employed for weighing the PKS, CNS, polyester resin, methyl-ethyl ketone peroxide and cobalt naphthalene were weighed. The percentage amount of the PKS and CNS weight composition was 72 wt.%, binder was 25 wt.% of polyester resin; while the hardener - cobalt naphthalene and the catalyst - methyl-ethyl ketone peroxide was 1.5 wt.%, respectively. Table 1 presents the weight percent (wt.%) composition of PKS to CNS, polyester resin, methyl-ethyl ketone peroxide and cobalt naphthalene.

Table 1. Weight percent composition of PKS/CNS/polyester resin in the biocomposite

Mixing Ratio (PKS/CNS)	PKS/CNS (wt.%)	PR (wt.%)	CN (wt.%)	MEKP (wt.%)	TOTAL (%)
1:0	72	25	1.5	1.5	100
2:1	72	25	1.5	1.5	100
1:1	72	25	1.5	1.5	100
1:2	72	25	1.5	1.5	100
0:1	72	25	1.5	1.5	100

*PR denotes Polyester resin, CN denotes Cobalt naphthalene, and MEKP denotes Methyl-ethyl ketone peroxide.

The PKS and CNS grains were blended at mixing ratios 1:0, 1:1, 1:2, 2:1 and 0:1 at a fixed weight composition of 72 wt.%, respectively, and separately stored in labelled zip-locked bags. The weighed resin, methyl-ethyl ketone peroxide and cobalt naphthalene were placed in a separate bowl and stirred to

obtain a uniform solution. The stored PKS and CNS in labelled zip-locked bags were transferred into the different uniform solution of the binder, hardener, and catalyst. The aggregate was quickly and thoroughly stirred at room temperature until a uniform mix was obtained. The resulting homogeneous aggregate was poured into the prepared moulds, compressed at a constant pressure of 18 MPa, carefully ejected and then, cured at a room temperature for 20 days, and further oven-cured at 100°C for 2 hours. The mould, made from mild steel because of its ease of machinability, availability, and considerable good corrosion resistance, had an internal diameter of 115 mm, depth of 72 mm, wall thickness of 10 mm and a piston hole of 22 mm. Figure 1 depicts the samples of produced resin-bonded palm kernel and coconut shell grain-based abrasive grinding wheels.

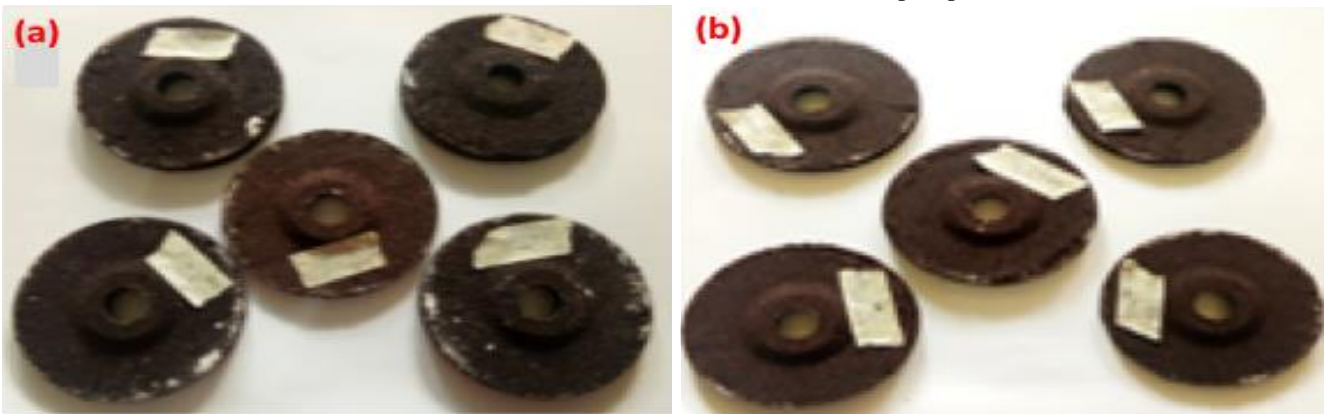


Figure 1. Samples of the produced grinding wheels of (a) 250 µm grain size and (b) 500 µm grain size

B. Characterisation of the produced grinding wheels

Microstructural analysis, water absorption testing, impact strength testing, flexural testing, hardness testing, and wear rate testing were performed on the produced resin-bonded palm kernel and coconut shell grain-based abrasive grinding wheels.

1) Microstructural evaluation

Due of their particle nature, the produced grinding wheel samples were not polished before the microstructure examination. To reveal their microstructural characteristics, the microscopic analysis was conducted on M50 and M250 magnification optical microscope images, captured with the use of an inbuilt camera (Ajimotokan *et al.*, 2022; Bello *et al.*, 2021). The produced grinding wheels were evaluated for grain distribution uniformity, and their physico-mechanical and tribological behaviour was further explained and affirmed through optical microstructural analysis.

2) Water absorption test

The weight of the produced grinding wheel samples before immersion in distilled water for 24 hours were measured, taken, and recorded. The samples were removed from the water, surface cleansed, and then reweight and recorded. Thus, the percentage water absorption of the produced abrasive grinding wheels was computed employing

the percentage weight differences as expressed using Eqn. 1 (Ibrahim *et al.*, 2019):

$$\% \text{ water absorption} = \frac{W_2 - W_1}{W_1} \times 100 \quad (1)$$

where W_2 denotes the final weight after immersion in water and W_1 is the initial weight before immersion in water.

3) Impact strength test

The impact strength test was conducted utilising an impact testing machine (ISOD6705U/33122). The testing of the produced grinding wheels was carried out based on standard testing procedure ASTM E23 (ASTM E23, 2018). Each prepared test specimen was placed and fastened to the grip, and a calibrated pendulum hammer of a predetermined velocity of 3.65 m/s with 150 and 300 Joules capacities were raised and released to hit the sample specimen.

The absorbed energy from the impact causes the specimen to break, and the deflected pendulum energy loss on the calibrated scale was taken and recorded. The impact strength was computed using Eqn. 2 (Abutu *et al.*, 2018):

$$s_i = \frac{E}{f} \quad (2)$$

where s_i denotes the impact strength, E is the absorbed energy, and f is the thickness of the specimen.

4) Flexural test

The flexural strength test, a test method for measurement of materials behaviour under simple beam loading, was conducted using a universal testing machine (Model: Testometric FS5080) based on standard test method ASTM D7264 (ASTM D7264, 2016). The applied load at the middle point of each prepared test specimen with a span length of 40 mm was carried out at a speed of 0.5 mm/min, and its findings were plotted on a stress-strain diagram. The flexural strength, a measure of the capability of a composite material to withstand applied bending forces to its longitudinal axis, was computed using Eqn. 3 (Tegegne & Shiferaw, 2020):

$$\sigma = F \times S = \frac{3PS}{2bt^2} \quad (3)$$

Where σ denotes flexural strength, P is the maximum test load, S is the span length between load points, b is the sample width, and t is the sample thickness.

5) Hardness test

The hardness test, a measure of the plastic deformation that the material can withstand under the influence of external stress, was conducted on the produced abrasive grinding wheel based on standard test method ASTM E18-20 (ASTM E18-20, 2020). The Rockwell hardness tester on 'B' scale (38506) with 1.56 mm steel ball indenter of 10 kg minor load, 100 kg major load, and 101.2 HRB standard block of hardness value at a pre-determined dwell time was employed for the hardness test. The hardness value of the sample is the distance between the baseline and the depth final measurements when transformed to a hardness number. The grinding wheel's hardness can be computed using Eqn. 4 (Obot *et al.*, 2017; Sa'ad *et al.*, 2021):

$$HR = E - e \quad (4)$$

Where E denotes a constant based on the indenter form and e is the permanent increase in the penetration depth because of the major load.

6) Wear rate test

The wear rate test of the abrasive grinding wheels was carried out using the TABER Pin on disk wear testing machine at two different temperatures based on standard test method ASTM G99-17 (ASTM G99-17, 2017) to understand the grinding wheels' wear behaviour under possible frictional heat in application. The wear rate of each samples was determined utilising a pin-on-disk machine through the sliding of the samples over a surface made of cast iron at various loads of 40, 80, 120, and 160 g, 2.4 m/s sliding speed, and a 20-minute holding time at different temperatures of 50°C and 150°C, respectively. The initial weight of each sample was taken, ran through a fixed sliding distance, and the sample was removed, cleaned and dried. The final weight of the sample was then taken to determine the weight loss due to abrasive wear. The measured weight differentials before and after the test gave the wear rate of the sample. The weight loss can be converted into wear rate using Eqn. 5 (Bashar, Peter, & Joseph, 2012; Edokpia *et al.*, 2016):

$$\text{Wear rate} = \frac{\Delta W}{S} = \frac{W_x - W_y}{S} \quad (5)$$

Where ΔW denotes the change in weight of the sample before and after the wear rate test, S is the total sliding distance, W_x is the initial weight of the sample before the test, and W_y is the final weight of the sample after the test.

III. RESULTS AND DISCUSSION

Figures 2, 3, and 4 depict the optical micrographs of the produced abrasive grinding wheels for 250, 500, and 850 μm grain sizes, respectively, in 50X and 250X magnified optical images. Because the grains are tightly packed, as observed in Figure 2, there is a stronger interfacial bond between the grain matrix and the binder. These tightly packed particles are a result of the grain size finest, which produces a high surface area to the volume of the binder, providing a closer and stronger binding. Additionally, the micrograph depicts that the grains maintained good alignment and low deformation with the resin matrix, providing strong resistance to wear due to grain pull-off effects (Obot *et al.*, 2017). Figures 3 and 4 were observed to have large pores, poor grain alignment, uneven protrusion, and poor abrasive distribution and orientation.

These characteristics can lead to surface defects, residual stress and grinding wheel deterioration, and premature abrasive grain chipping (Aurich *et al.*, 2013; Li & Axinte, 2016).

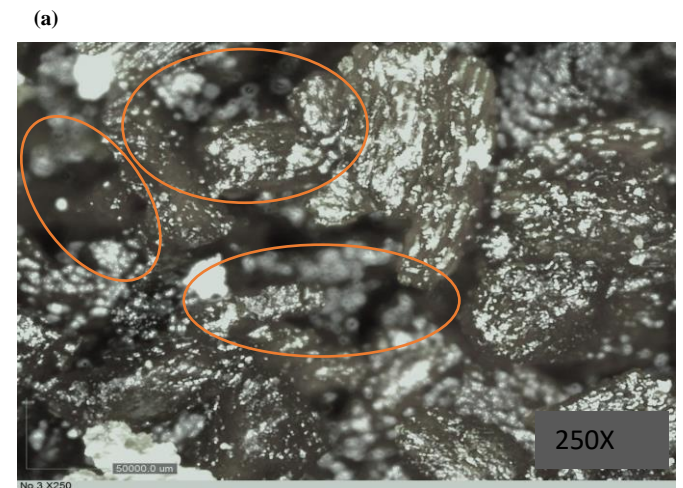
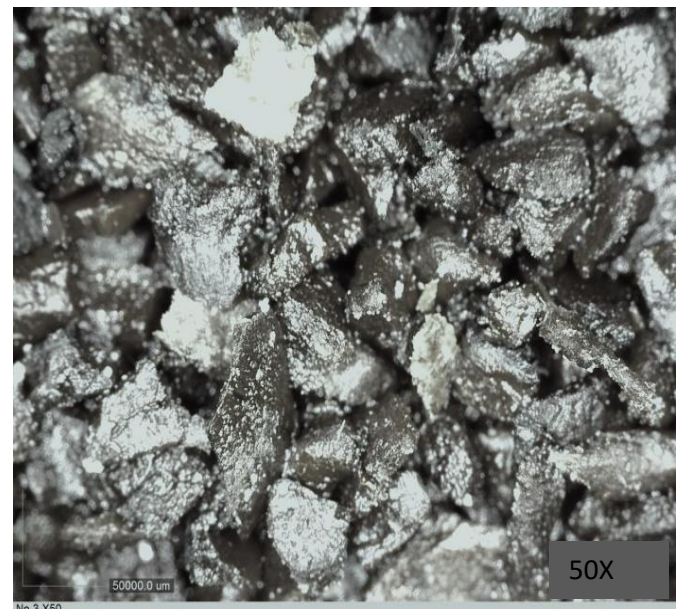
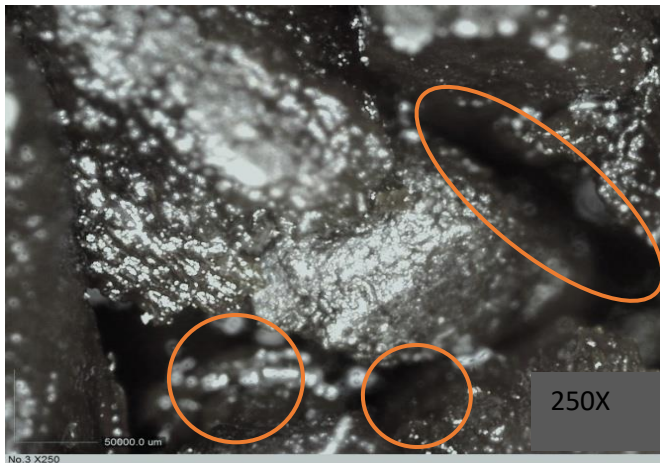


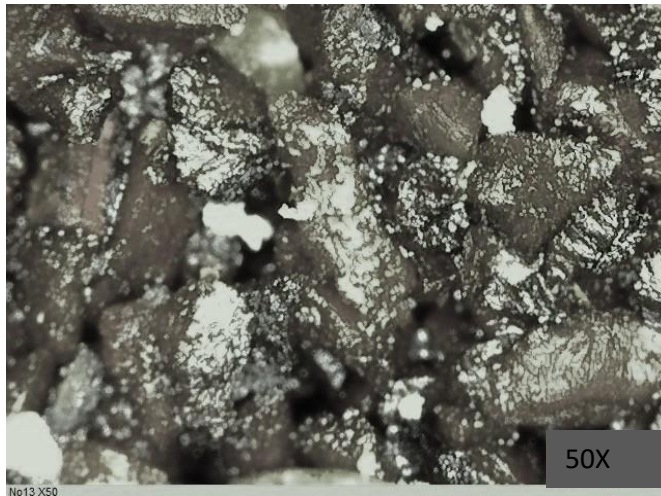
Figure 2. Optical micrograph of the abrasive grinding wheel for 250 μm particle size: Magnification a.) 50X and b.) 250X



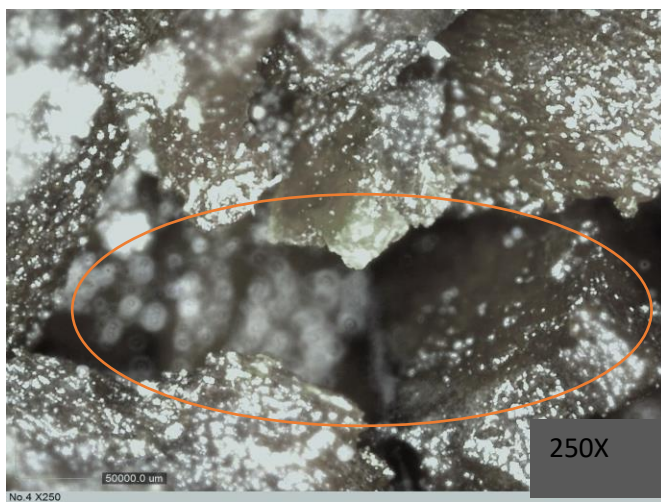
(a)



(b) Figure 3. Optical micrograph of the abrasive grinding wheel for 500 μm particle size: Magnification a.) 50X and b.) 250X



(a)



(b) Figure 4. Optical micrograph of the abrasive grinding wheel for 850 μm particle size: Magnification a.) 50X and b.) 250X

Figure 5 depicts how variations in grain size and mixing ratio affect the water resistance of the produced abrasive grinding wheels. As the grain sizes increased from 250 to 850 μm, the rates of water absorption by the abrasive grinding wheels increased, which can be attributed to a weakening of the interfacial connection between the binder and grain components, causing pores enlargement and porosity. In addition, PKS and CNS, which are biocomposite grain-based abrasives, have strong hydrophilic properties with numerous hydroxyl groups (-OH) in their fibres, making them to have low water resistance (Ibrahim *et al.*, 2019; Sa’ad *et al.*, 2021). This peculiar naturally strong hydrophilic property attributes of the PKS and CNS enhances water uptake by these lignocellulosic materials because of the hydrogen bond formation between the fillers and water molecules, which compared favourably with findings reported by Odior and Oyawale, (2011); Ibrahim *et al.*, (2019); and Sa’ad *et al.*, (2021). Furthermore, the aggregates with higher PKS demonstrated improved resistance to water soaking effects. This particular quality of the abrasive grinding wheel might be due to particulate nature of the parent material, which was also established by the hardness results.

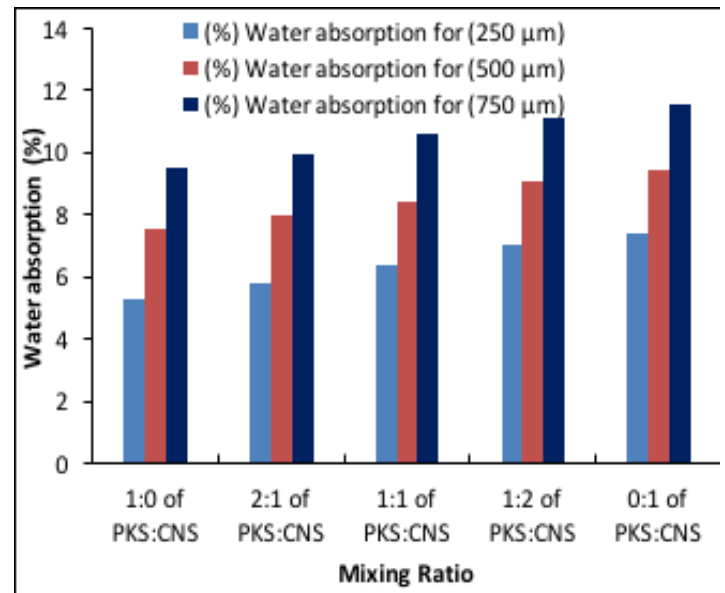


Figure 5. The effects of grain size and mixing ratio on the rate of water absorption of the abrasive grinding wheels

Figure 6 depicts the effects of grain size and mixing ratio on the impact strength of the produced abrasive grinding wheels. The impact strength of the grinding wheels varied from 73.3 to 90 J/m. The highest resistance was exhibited by the grinding wheel made of pure CNS with 250 μm grain size, while the lowest resistance was exhibited by the sample made of pure PKS with 850 μm grain size. With a reduction in particle size and an increase in CNS content in the aggregates, the resistance to impact by abrasive grinding wheels increased. This may be due to the smaller grains' matrix having greater interfacial bonding, as well as the fact that wheels made of higher CNS grain content offers better resistance to impact (Ibrahim *et al.*, 2019; Sa’ad *et al.*, 2021).

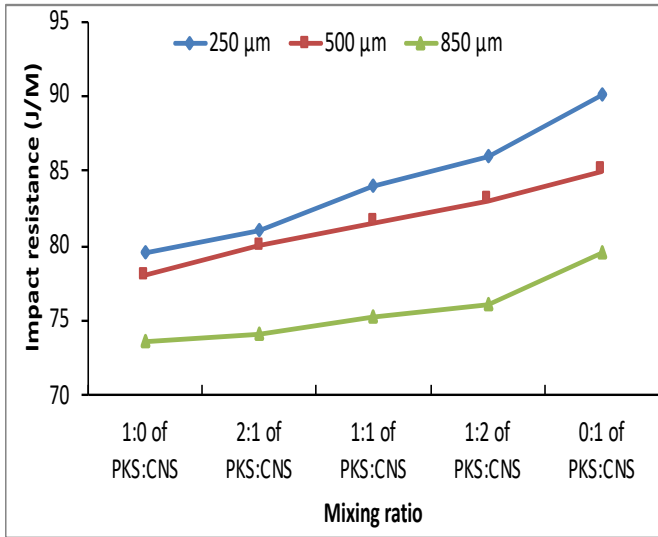


Figure 6. The effects of grain size and mixing ratio on impact strength of the abrasive grinding wheels

Figure 7 depicts the effects of grain size and mixing ratio on the flexural strength of the produced grinding wheels. The flexural strength of the abrasive grinding wheels varied from 3.94 to 5.46 MPa. The produced grinding wheel from the pure CNS with 850 μm grain size had the least flexural strength, 3.94 MPa, and the abrasive grinding wheel made from pure PKS with 250 μm grain size had the most flexural strength, 5.46 MPa. With a reduction in grain size and an increase in CNS concentration in the aggregates, the flexural strength increased and decreased respectively. These can be as a result of high grain packing, coordinated grain alignment, and stronger interfacial matrix bonded structure (Tegegne & Shiferaw, 2020).

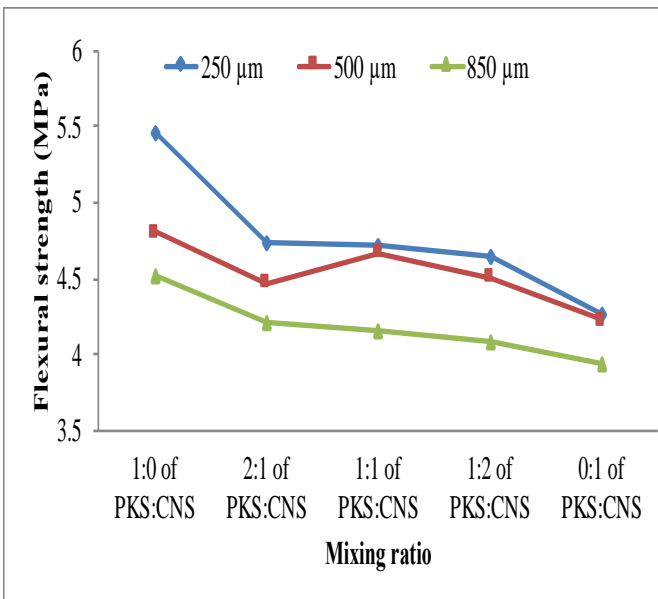


Figure 7. The effects of grain size and mixing ratio on flexural strength of the abrasive grinding wheel

Figure 8 depicts the effects of variation in grain size and mixing ratio on the Rockwell hardness values of the produced grinding wheels. The hardness values of the abrasive grinding wheels varied from 6.42 to 9.32 HRB. The produced grinding wheel from pure PKS with 850 μm grain size exhibited the lowest value, 6.42 HRB, and the grinding wheel made from pure CNS with 250 μm grain size exhibited the highest value, 9.32 HRB. According to Sa'ad *et al.* (2021) grain packing and a stronger interfacial bound matrix structure may be attributed to the enhanced hardness of the abrasive grinding wheels with smaller grains and higher CNS concentrations in the aggregates. Similar findings were reported by Obot, Yawas and Aku, (2016) and Ibrahim *et al.* (2019) that the hardness of grain-based sandpaper from agro-residues decreased with an increase in the grain size.

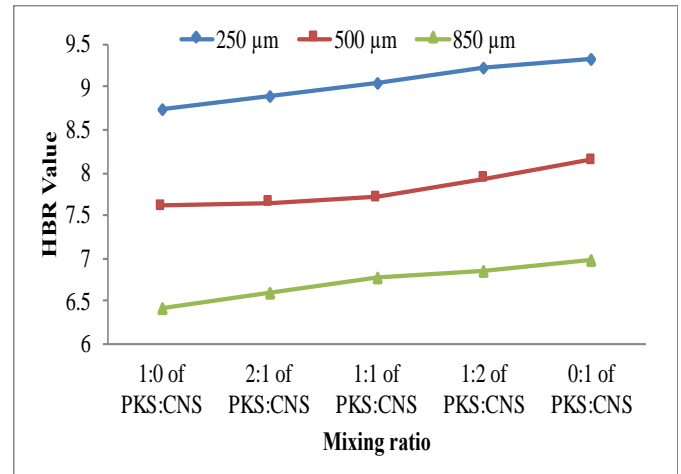


Figure 8. The effects of grain size and mixing ratio on Rockwell hardness of abrasive grinding wheels

Figures 9 to 14 depict the effects of variation in grain size and mixing ratio on the wear rate of the produced grinding wheels at 50°C and 150°C under various loads of 40, 80, 120, and 160 g, respectively. The wear resistance of the abrasive grinding wheels varied from 0.44 to 2.08 mg/m at 50°C and 1.6 to 2.87 mg/m at 150°C across the 250, 500 and 850 μm grain sizes, respectively. Figures 11 and 14 depicted that the wheels made from 850 μm at 50°C and 150°C, respectively, and at same fixed load of 160 g exhibited the highest wear rates of 2.08 and 2.87 mg/m respectively. Figures 9 and 12 depicted that wheels made from 250 μm at 50°C and 150°C, respectively, and at same load of 40 g exhibited the least wear rates of 0.44 and 1.6 mg/m respectively. On the produced grinding wheels, the wear rate increased as the operating temperature and applied loads increased, and it reduced when the grain sizes, applied loads, and operating temperature decreased. This is because the composite's resin's binding ability has begun to degrade at higher temperatures. The grinding wheel made from pure PKS of 250 μm grain size exhibited the least wear rate of 0.44 mg/m; i.e., offering the highest wear performance. Better interfacial bond between the grain matrix and the resin may have contributed to the decrease in wear rate with smaller grains by lowering the likelihood of grain pull-out, which can increase the wear rate (Koya & Fono-Tamo, 2013; Olele *et al.*, 2016; Zhang *et al.*, 2021).

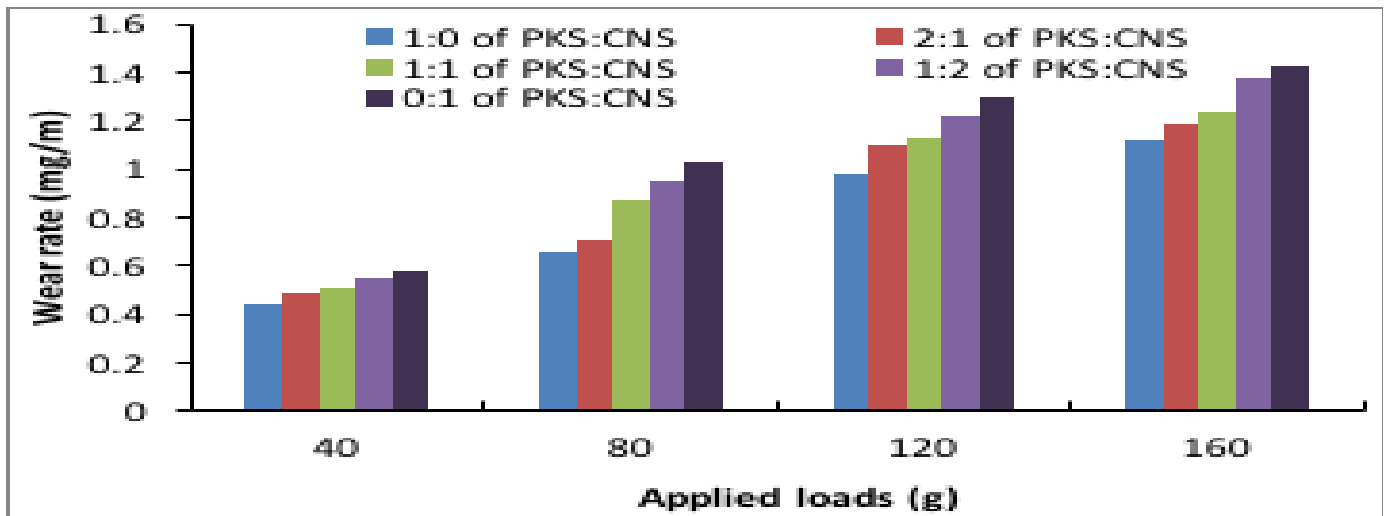


Figure 9. The effects of variation in grain size and mixing ratio on the wear rate of 250 μm abrasive grinding wheels at 50°C under various loads

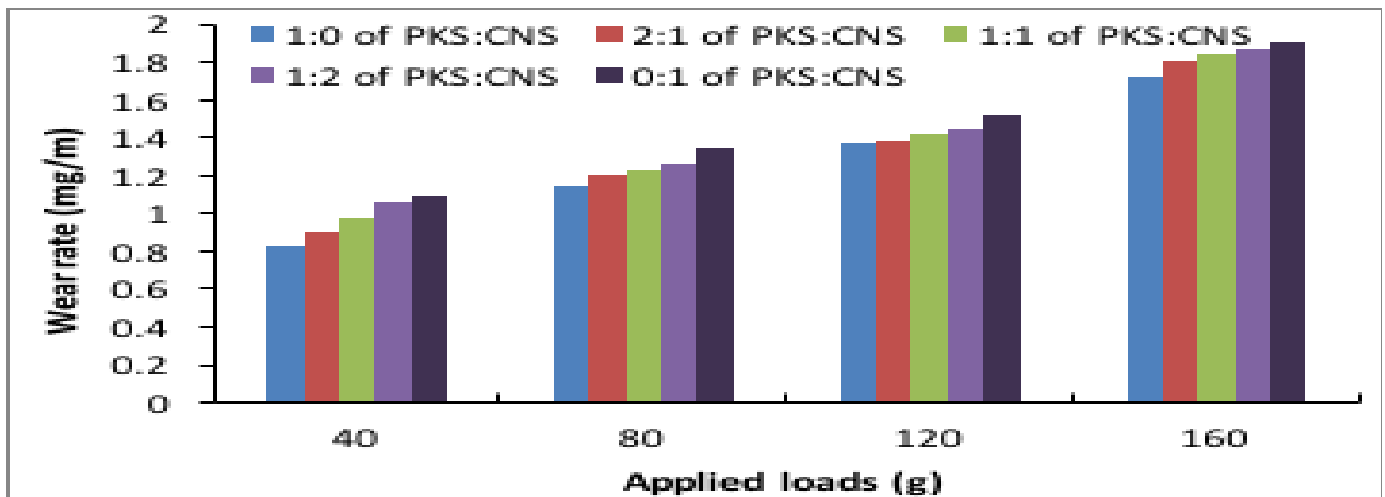


Figure 10. The effects of variation in grain size and mixing ratio on the wear rate of 500 μm abrasive grinding wheels at 50°C under various loads

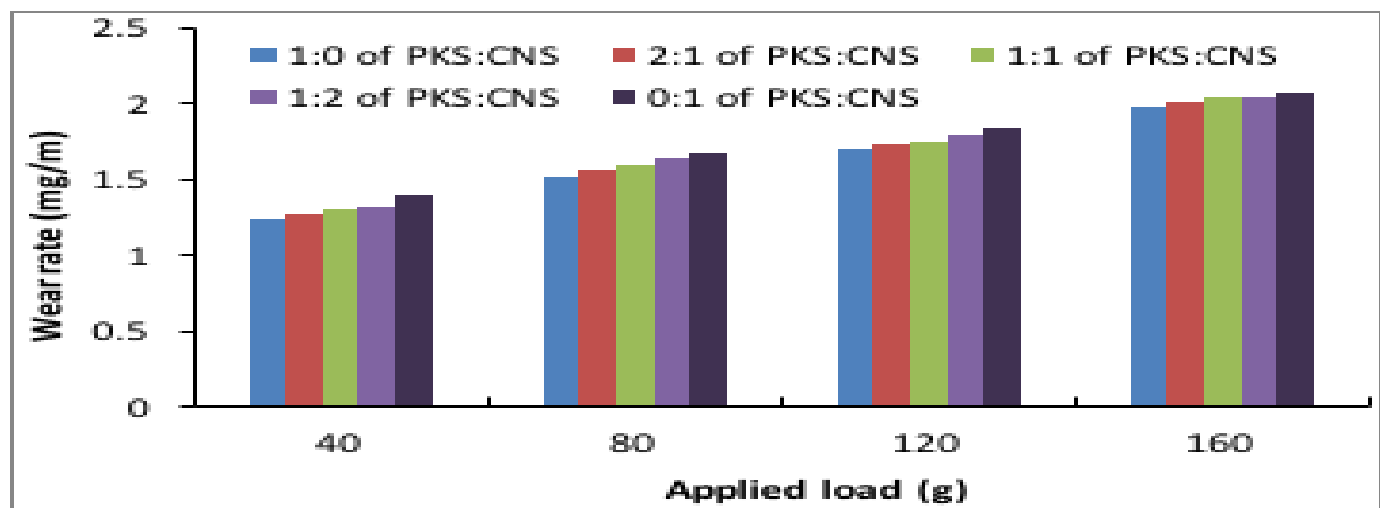


Figure 11. The effects of variation in grain size and mixing ratio on the wear rate of 850 μm abrasive grinding wheels at 50°C under various loads

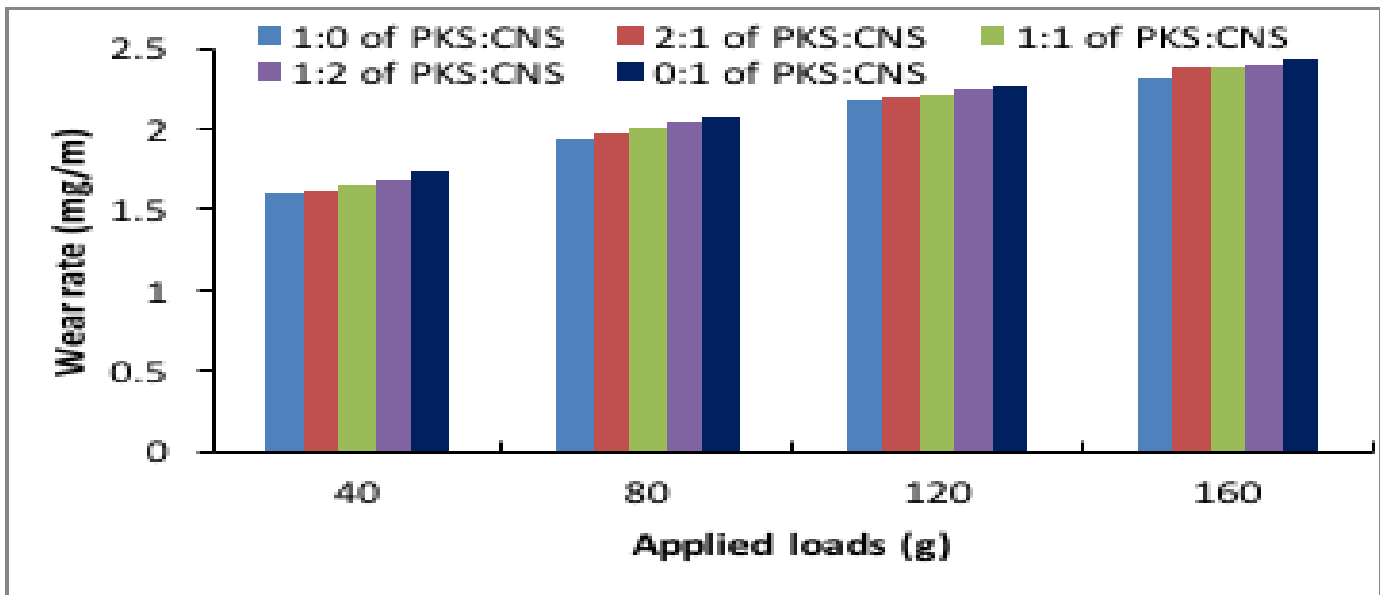


Figure 12. The effects of variation in grain size and mixing ratio on the wear rate of 250 μm abrasive grinding wheels at 150°C under various loads

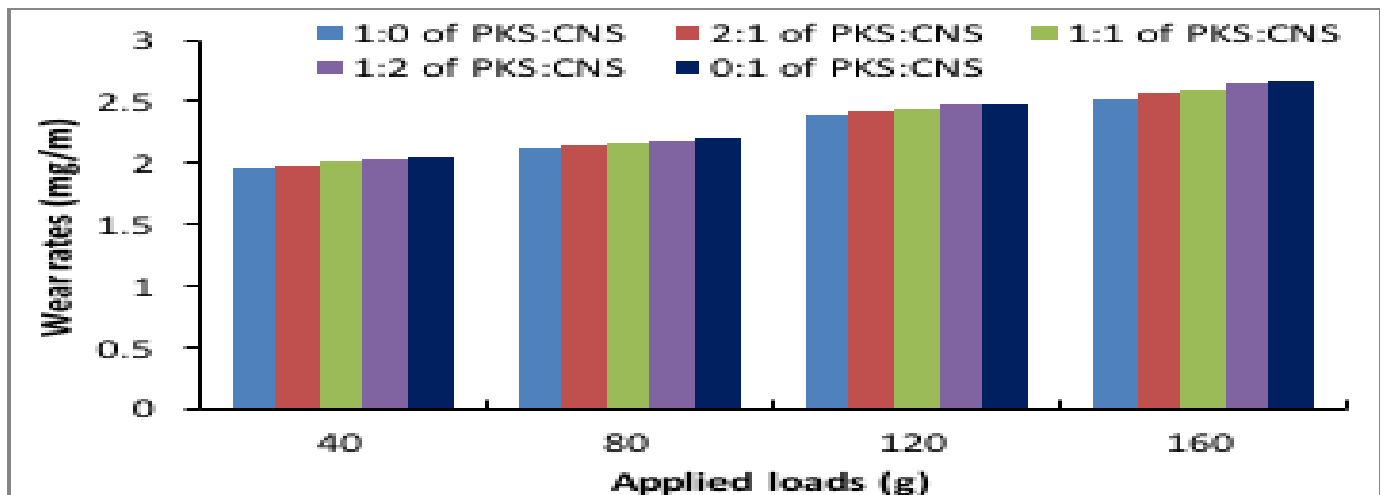


Figure 13. The effects of variation in grain size and mixing ratio on the wear rate of 500 μm abrasive grinding wheels at 150°C under various loads

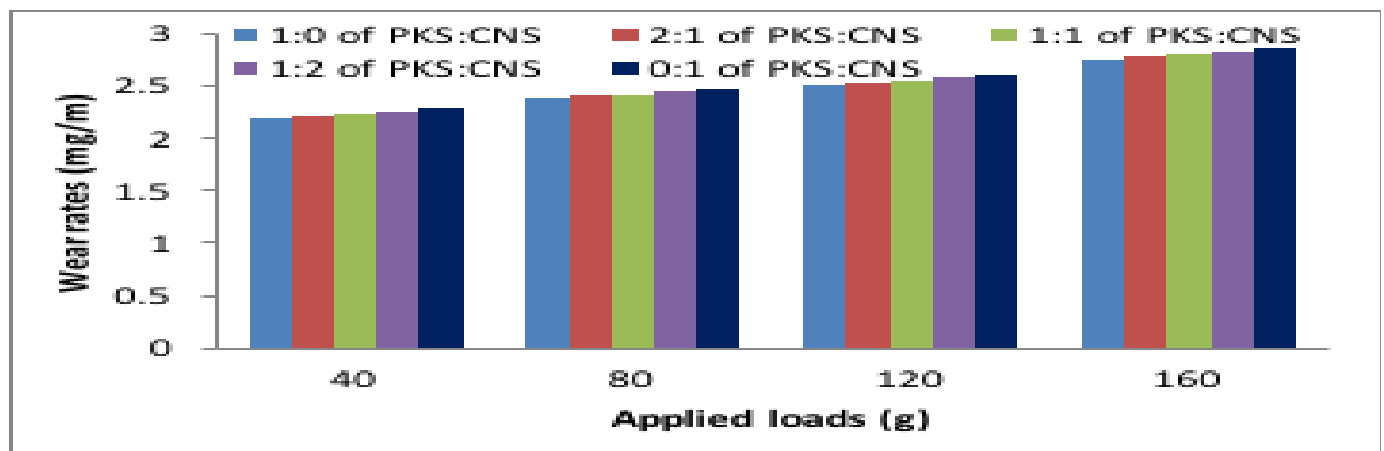


Figure 14. The effects of variation in grain size and mixing ratio on the wear rate of 850 μm abrasive grinding wheels at 150°C under various loads

IV. CONCLUSION

This study examined the morphology and microstructural evolution of resin-bonded palm kernel shell (PKS) and coconut shell (CNS) grain-based abrasive grinding wheels and their physico-mechanical and tribological properties. The PKS and CNS microstructural evolution, grain size variation, and mixing ratio in the abrasive grinding wheels significantly influenced the properties investigated. A decrease in grain sizes led to an increase in the hardness value, flexural strength, and impact resistance. An increase in grain sizes led to an increase in the water absorption percentage and wear rate of the grinding wheels. The grinding wheels containing pure PKS had the lowest hardness value (6.42 HRB) and wear rate (0.44 mg/m). For grain sizes of 250, 500, and 850 μm , respectively, the pure CNS had the highest water absorption percentages of 7.42%, 9.47%, and 11.58%. The resulting abrasive grinding wheels' microstructure, physico-mechanical and tribological properties suggest that they could possibly be considered for usage as abrasive grinding wheels, in particular for wood cutting and finishing processes.

AUTHOR CONTRIBUTIONS

A. A. Samuel: Conceptualisation, Development and Characterisation, and Writing - Draft Preparation and Final Editing. **A. Sulaiman:** Development and Characterisation, and Writing - Draft Preparation and Final Editing. **H. A. Ajimotokan:** Visualisation, Supervision, and Writing - Reviewing and Editing. **S. E. Ibitoye:** Development and Characterisation. **T. K. Ajiboye:** Writing - Reviewing and Editing. **T. S. Ogedengbe:** Writing - Draft Preparation, Reviewing and Editing, and Final Editing. **I. O. Alabi:** Writing - Draft Preparation and Final Editing.

REFERENCES

- Abutu, J.; S. A. Lawal, Ndaliman, M. B., Lafia-Araga, R. A., Adedipe, O., and Choudhury, I. A. (2018).** Effects of process parameters on the properties of brake pad developed from seashell as reinforcement material using grey relational analysis. *Engineering Science and Technology, an International Journal*, 21(4), 787–797. <https://doi.org/10.1016/j.jestch.2018.05.014>
- Ajimotokan, H. A., Samuel, A. A., Ajiboye, T. K., Ogedengbe, T. S., and Alabi, I. O. (2022).** Morphology and physico-mechanical properties of resin-bonded palm kernel shell and coconut shell grain-based sandpaper composites. *Nigerian Journal of Technological Development*, 19(4), 268–276. <http://dx.doi.org/10.4314/njtd.v19i4.11>
- Ajimotokan, H. A. and Samuel, A. A. (2020).** Process for making bio-composite abrasive grinding wheel. *Patent Number: NG/P//2020/186*. Abuja, Nigeria: National Office of Technology Acquisition and Promotion.
- ASTM D7264. (2016).** Flexural properties of composites. West Conshohocken, USA: ASTM International.
- ASTME11-20. (2020).** Standard specification for woven wire sieve cloth and test sieves. West Conshohocken, USA: ASTM International. <https://doi.org/10.1520/E0011-20>
- ASTM E18-20. (2020).** Standard test methods for Rockwell hardness of metallic materials. West Conshohocken, USA: ASTM International. <https://doi.org/10.1520/E0018-20>
- ASTME23. (2018).** Standard test method for notched bar impact testing of metallic materials. West Conshohocken, USA: ASTM International.
- ASTM G99-17. (2017).** Standard test method for wear testing with a pin-on-disc apparatus. West Conshohocken, USA: ASTM International. <https://doi.org/10.1520/G0099-17>
- Aurich, J. C.; B. Linke; M. Hauschild; M. Carrella and B. Kirsch. (2013).** Sustainability of abrasive processes. *CIRP Annals - Manufacturing Technology*, 62(2), 653–672. <https://doi.org/10.1016/j.cirp.2013.05.010>
- Bashar, D. A.; B. M. Peter and M. Joseph. (2012).** Material selection and production of a cold-worked composite brake pad. *World Journal of Engineering and Pure and Applied Science*, 2(3), 1–5.
- Bello, K. A., Abdullahi, U., Abajo, A. S., Adebisi, A. A., Dodo, M. R., Abdulwahab, M., and Adeleke, S. A. (2021).** Optimizing tensile properties of age hardened A356 aluminium alloy via Taguchi method. *Nigerian Journal of Engineering*, 28(1), 61–68.
- Bratan, S., Roshchupkin, S., and Novikov, P. (2017).** Modeling the grinding wheel working surface state. In *Procedia Engineering* (Vol. 206, pp. 1419–1425). <https://doi.org/10.1016/j.proeng.2017.10.655>
- Durowaye, S. I., Lawal, G. I., Akande, M. A., and Durowaye, V. O. (2014).** Mechanical properties of particulate coconut shell and palm fruit polyester composites. *International Journal of Materials Engineering*, 2014(4), 141–147. <https://doi.org/10.5923/j.ijme.20140404.04>
- Edokpia, R. O., Aigbodion, V. S., Atuanya, C. U., Agunsoye, J. O., and Mu'azu, K. (2016).** Experimental study of the properties of brake pad using egg shell particles–Gum Arabic composites. *Journal of the Chinese Advanced Materials Society*, 4(2), 172–184. <https://doi.org/10.1080/22243682.2015.1100523>
- Federation of European Producers of Abrasives. (2020).** P-grit sizes coated abrasive products. Retrieved from <http://www.fepa-abrasives.org/Abrasiveproducts/Grains/Pgritsizescoated.aspx>. accessed: 18.11.2020
- Godino, L., Pombo, I., Sanchez, J. A., and Alvarez, J. (2018).** On the development and evolution of wear flats in microcrystalline sintered alumina grinding wheels. *Journal of Manufacturing Processes*, 32, 494–505. <https://doi.org/10.1016/j.jmapro.2018.03.023>
- Ibrahim, H. K., Abdulhamid, A. S., Shuaib-Babata, Y. L., Popoola, O. T., Kareem, A. G., Adeyi, A.M., Busari, O. Y., and Ambali, I. O. (2019).** Development of abrasive sandpaper grains from agro-waste material for polishing of wood surface. *Engineering and Technology*, 2(1), 48–60.
- Kohli, R. (2016).** Microabrasive Technology for Precision Cleaning and Processing. In *Developments in Surface Contamination and Cleaning: Second Edition* (Vol. 1, pp. 627–666). <https://doi.org/10.1016/B978-0-323-29960-2.00014-9>
- Koya, O. A. and Fono-Tamo, R. S. (2013).** Evaluation of mechanical characteristics of friction lining from agricultural waste. *International Journal of Advancements in Research & Technology*, 2(11), 1–5.

- Li, H. N. and Axinte, D. (2016).** Textured grinding wheels: A review. *International Journal of Machine Tools and Manufacture*, 109, 8–35. <https://doi.org/10.1016/j.ijmachtools.2016.07.001>
- Obot, M.U., Yawas, D. S., and Aku, S. Y. (2016).** An assessment on the production of abrasive sandpaper from locally sourced materials. *Tribology in Industry*, 38(2), 176–185.
- Obot, Mfon Udo, Yawas, D. S., and Aku, S. Y. (2017).** Development of an abrasive material using periwinkle shells. *Journal of King Saud University - Engineering Sciences*, 29(3), 284–288. <https://doi.org/10.1016/j.jksues.2015.10.008>
- Odior, A. O. and Oyawale, F. A. (2011).** Formulation of silicon carbide abrasives from locally sourced raw materials in Nigeria. In *Proceedings of the World Congress on Engineering 2011, WCE 2011* (Vol. 1, pp. 787–791).
- Olele, P. ., Nkwocha, A. ., Ekeke, I. ., Ileagu, M., and Okeke, E. (2016).** Assessment of palm kernel shell as friction material for brake pad production. *International Journal of Engineering and Management Research*, 6(1), 281–284.
- Ratia, V., Heino, V., Valtonen, K., Vippola, M., Kemppainen, A., Siitonen, P., and Kuokkala, V. T. (2014).** Effect of abrasive properties on the high-stress three-body abrasion of steels and hard metals. *Tribologia*, 32(1), 3–18.
- Sa'ad, H., Omoleiyomi, B. D., Alhassan, E. A., Ariyo, E. O., and Abadunmi, T. (2021).** Mechanical performance of abrasive sandpaper made with palm kernel shells and coconut shells. *Journal of the Mechanical Behavior of Materials*, 30(1), 28–37. <https://doi.org/10.1515/jmbm-2021-0004>
- Samuel, A. A. (2019).** *Development and physico-mechanical characterisation of abrasive grinding wheels from coconut and palm kernel shells*. University of Ilorin, Ilorin, Nigeria.
- Sauget, A., Zhou, X., and Pizzi, A. (2014).** Tannin-resorcinol-formaldehyde resin and flax fiber biocomposites. *Journal of Renewable Materials*, 2(3), 173–181. <https://doi.org/10.7569/JRM.2013.634128>
- Senthilkumar, K., Saba, N., Rajini, N., Chandrasekar, M., Jawaid, M., Siengchin, S., and Alotman, O. Y. (2018).** Mechanical properties evaluation of sisal fibre reinforced polymer composites: A review. *Construction and Building Materials*, 174, 713–729. <https://doi.org/10.1016/j.conbuildmat.2018.04.143>
- Suresh, S., Sudhakara, D., and Vinod, B. (2020).** Investigation on industrial waste eco-friendly natural fiber-reinforced polymer composites. *Journal of Bio- and Tribo-Corrosion*, 6(2), 1–14. <https://doi.org/10.1007/s40735-020-00339-w>
- Tegegne, A. and Shiferaw, M. (2020).** Experimental of Flexural and Hardness Property of Palm-Sisal Reinforced Epoxy Resin Hybrid Composite Materials. *International Journal of Research and Scientific Innovation*, VII(I), 143–153.
- Zhan, G. D., Wang, P., and Wang, L. (2021).** Defining the true hardness of materials harder than single crystal diamond. *Research Square*, 1–15. <https://doi.org/10.21203/rs.3.rs-614606/v1>
- Zhang, J., Liu, B., Zhou, Y., Essawy, H., Li, J., Chen, Q., and Du, G. (2021).** Preparation and performance of tannin-glyoxal-urea resin-bonded grinding wheel loaded with SiO₂ reinforcing particles. *Maderas: Ciencia Tecnologia*, 23(48), 1–16. <https://doi.org/10.4067/s0718-221x2021000100448>
- Zhang, J., Luo, H., Pizzi, A., Du, G., and Deng, S. (2015).** Preparation and characterization of grinding wheels based on a bioresin matrix and glass sand abrasives. *BioResources*, 10(3), 5369–5380. <https://doi.org/10.15376/biores.10.3.5369-5380>